

Theoretical Study of Indirect Heating Temperature Swing Adsorption in an Adsorbent Coated Finned Tube Heat Exchanger

Mohsen Gholami

Department of Chemical Engineering, Faculty of Engineering, University of Isfahan, Isfahan, Iran

Article History

Received: 2017-09-17

Revised: 2018-05-28

Accepted: 2018-05-30

Abstract

In this study, the performance of an adsorbent coated finned tube exchanger for carbon capture was investigated numerically. The results showed that this structure has a great potential for being applied as a medium for CO₂ capture by rapid indirect thermal swing adsorption. By using this structure, the recovery of 96%, and purity of 98% were achieved with a simple cycle consisting of two steps, including adsorption and regeneration. To assess the effect of operating parameters, the cooling water temperature, hot water temperature and feed flow rate were selected as varying parameters, and the recovery and purity were selected as objective functions. The results showed that by increasing the cooling water temperature from 25 C to 45 C the recovery decreases from 65% to 61% while the reduction of purity is almost negligible. The heating temperature has a more intense effect on the recovery and purity. By increasing the heating temperature from 80 to 120 the recovery increases from 16% to 65% and purity increases from 92% to 98%. The variation of feed flow rate showed that by increasing the feed from 2 to 6 (STP CM/min) the recovery decreases from 98.5% to 65% and the purity increases from 96% to 98%. It should be noted that finned tube exchangers are well developed to create minor pressure drop. Thus, they are suitable structures for getting coated by adsorbent for the purpose of gas separation by Rapid Thermal Swing Adsorption.

Keywords

Finned tube; Coated exchanger; Rapid Thermal Swing Adsorption; CO₂ capture

1. Introduction

The massive usage of fossil fuels in the recent century has caused global warming. The forecasted destructive outcome of this climate change has convinced many governments to find a way to control the rate of greenhouse gas emission. In recent years, many researches around the world have been focused on adsorption process to capture the CO₂. Most of these researches have dealt with synthesizing an appropriate adsorbent. Although there are lots of published papers on developing a wide variety of adsorbents, most of them have something in common: selective CO₂ adsorption by an amine functional group which is grafted or impregnated inside a porous solid support. It means that carbon dioxide is chemically adsorbed by the functional groups of adsorbent; thus, the adsorption process supposedly proper for such a situation is Temperature Swing Adsorption. However, while designing a TSA cycle for such a

separation, a technical problem arises, that is cycle time. Because the rate of heat transfer in porous particles is low, the regeneration step in traditional TSA cycles lasts at least two hours, which requires a larger bed. To overcome this problem, some researches were focused on improving the traditional adsorption processes. In some researches, the granular adsorbents were heated indirectly in an exchanger type structure (Clause, Merel, & Meunier, 2011; Lee & Sircar, 2008; Merel, Clause, & Meunier, 2008; Mérel, Clause, & Meunier, 2006). Although in this case the purity of separated CO₂ was high, the regeneration time wasn't short enough. In some researches, the adsorption cycle was modified to improve the economy of CO₂ capture (Hefti, Joss, Bjelobrck, & Mazzotti, 2016; Joss, Gazzani, & Mazzotti, 2017; Marx, Joss, Hefti, & Mazzotti, 2016). Despite the fact that the indirect heating and cycle modification are to some extent successful to

* Corresponding Author.

Authors' Email Address:

M. Gholami (mgholami_ui@yahoo.com),

ISSN (Online): 2345-4172, ISSN (Print): 2322-3251

© 2017 University of Isfahan. All rights reserved

reduce the regeneration time, they need a multiple bed system for separation which should be executed by a complicated system of valves and piping. Another improvement toward reducing regeneration time is a specialized form of indirect thermal heating in which the adsorbent is coated on the surface of a heat exchanger; in this case a new name has been coined for the process: Rapid Temperature Swing Adsorption, abbreviated to RTSA (Bonnissel, Luo, & Tondeur, 2001; Determan, Hoysall, & Garimella, 2012; Fatemeh Hosseini et al., 2017; R. Lively, Chance, Koros, Deckman, & Kelley, 2012; R. P. Lively et al., 2009; Rezaei et al., 2014). In 2001, Bonnissel et.al. coated the surface of a peltier cell by activated carbon, and reduced the cycle time to 20 minutes. In 2009- 2014, in Georgia institute of technology, a research was conducted to load the amine grafted adsorbent in the body of hollow fiber. In spite of the fact that the researchers were successful to reduce the cycle time to less than 3 minutes, applying hollow fiber as the medium for indirect heating has its own drawbacks: the complicated process of producing adsorbent loaded hollow fibers and high pressure drop of flowing water through hollow fibers.

The idea of adsorbent loaded hollow fiber for CO₂ capture is fascinating, but the hollow fiber itself is designed for low velocity flows. Though the idea of applying adsorbent coated exchangers for CO₂ capture has not been well investigated yet, the adsorbent coated exchangers have extensively been studied in adsorption refrigeration technology (Bauer, Herrmann, Mittelbach, & Schwieger, 2009; Boelman, Saha, & Kashiwagi, 1995; Freni et al., 2015; Restuccia, Freni, Russo, & Vasta, 2005; Yong & Wang, 2007; Zhu, Han, Lin, & Yu, 1992). Generally, for this purpose the adsorbent is coated on the external surface of a

finned tube exchanger made of copper or aluminum. In this case, the water easily flows through the pipes, and transfers the heat between water and the adsorbents through the fins. It should be noted that different kinds of these exchangers are commercially available. The successful application of coated exchangers for the purpose of chilling by SorTtech and AQSOA is a motivation to test this structure for the purpose of CO₂ separation. Therefore, the aim of this paper is to numerically assess the performance of adsorbent coated finned tube exchanger for capturing the CO₂ from a simulated flue gas.

2. Process Description

The schematic diagram of an adsorbent coated finned tube exchanger is shown in figure 1. As it is shown in this figure, a thin layer of adsorbent is coated on the fins of the exchanger. In the adsorption step, a gas consisting of N₂ and CO₂ enters the fin side of the exchanger, and the carbon dioxide is adsorbed on the adsorbent layer. The heat of adsorption is dissipated by the cooling water inside the tubes through the fins. The cooling water enters from one side of exchanger and exits from the other side with gas crossflowing it. In regeneration step, the hot water flows through the tubes that cold water passes in adsorption step. This hot water heats up the adsorbent layer leading to the extraction of high purity carbon dioxide from the adsorbents. In regeneration step the end of exchanger is closed and desorbed gas exits from the beginning of the bed. A schematic diagram of adsorption and desorption steps is shown in figure 2. To have a continues flow, it is necessary to have at least 2 beds in parallel, one in adsorption step and the other in regeneration step.

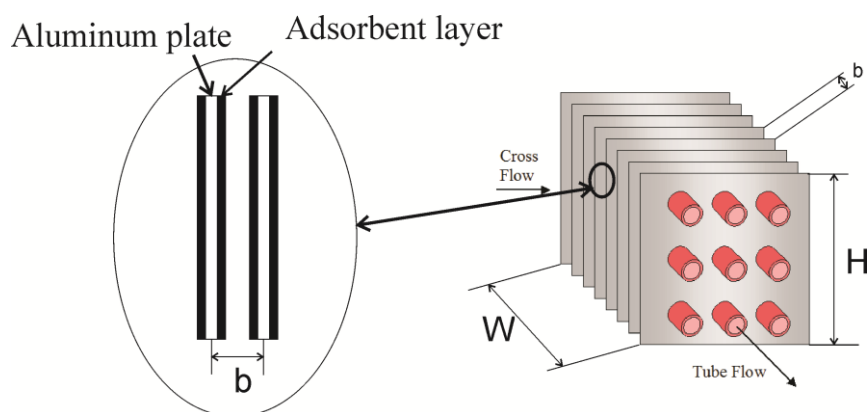


Figure.1. schematic diagram of an adsorbent coated finned tube exchanger

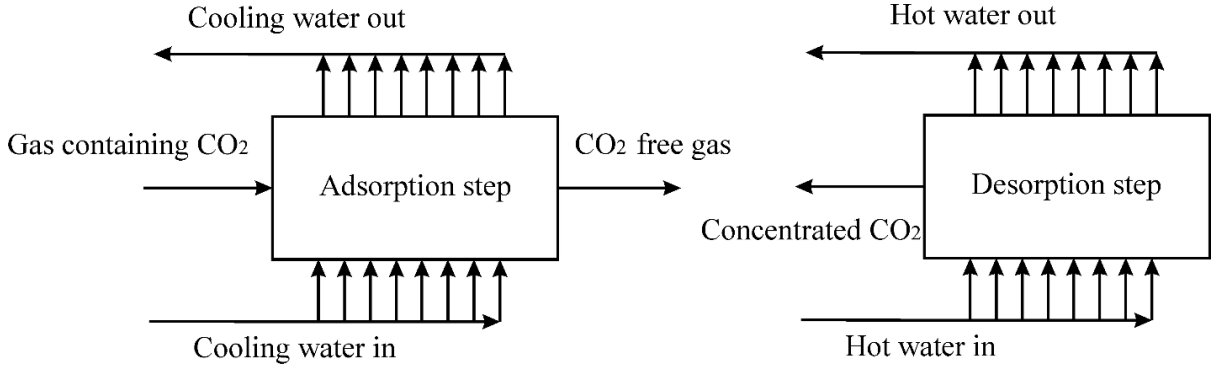


Figure 2. schematic representation of adsorption and desorption step

3. Mathematical Model

3.1. Assumptions and Limitations:

The mathematical model was developed based on the following assumptions:

1. Pressure is constant through the bed.
2. The flow pattern is described by the plug-flow model.
3. The gas consists of N_2 and CO_2 .
4. Only CO_2 is adsorbed by the adsorbent.

3.2. Conservation of Mole

Applying the conservation law of mass on a differential control volume of the adsorption bed results in:

$$\frac{1}{A_b \varepsilon_b} \frac{\partial(Qy)}{\partial z} + \frac{(1 - \varepsilon_b - \varepsilon_m)}{\varepsilon_b} \frac{\partial q}{\partial t} = - \frac{\partial}{\partial t} \left(y \frac{P}{RT^g} \right) \quad (1)$$

This equation was used to obtain the concentration profile along the exchanger. In the above equation, q , which is the average amount of material adsorbed per unit volume of the adsorbent, can be calculated by modified LDF model (Rezaei et al., 2014):

$$\frac{\partial q}{\partial t} = K_{s0} \exp(-\alpha\theta) (q^* - q) \quad (2)$$

where q^* is the equilibrium amount of adsorbed carbon dioxide and is calculated from the Toth isotherm.

$$q^* = \rho_{adsorbent} q_s \frac{bP}{\left(1 + (bP)^n\right)^{\frac{1}{n}}} \quad (3)$$

The saturation capacity and adsorption affinity are temperature-dependent parameters and can be calculated using the following correlations (Rezaei et al., 2014):

$$q_s = q_{s0} \exp\left(\eta \left(1 - \frac{T}{T_0}\right)\right) \quad (4)$$

$$b = b_0 \exp\left(\frac{-\Delta H}{RT_0} \left(1 - \frac{T_0}{T}\right)\right) \quad (5)$$

$$n = A + B \left(1 - \frac{T_0}{T}\right) \quad (6)$$

Due to the adsorption and desorption, the net molar flow rate through the bed varies with time and position. The net flow rate is calculated by applying total mole balance along the bed.

$$\frac{-1}{A_b \varepsilon_b} \frac{\partial Q}{\partial z} - \frac{(1 - \varepsilon_b - \varepsilon_m)}{\varepsilon_b} \frac{\partial q}{\partial t} = \frac{\partial}{\partial t} \left(\frac{P}{RT^g} \right) \quad (7)$$

3.3. Gas phase Conservation of Energy:

Due to the exothermic nature of adsorption, the temperature changes along the bed. The conservation of energy is used to calculate the temperature along the bed.

$$\begin{aligned} & -y \frac{Q}{\varepsilon_b A_b} c_p^{CO_2} \frac{\partial T^g}{\partial z} - (1-y) \frac{Q}{\varepsilon_b A_b} c_p^{N_2} \frac{\partial T^g}{\partial z} - \frac{1 - \varepsilon_b - \varepsilon_m}{\varepsilon_b} \left[\frac{\partial q}{\partial t} \int_{T^g}^{T^s} c_p^{CO_2} dT \right] \delta_k \\ & - \frac{2hH}{\varepsilon_b A_b} (T^g - T^a) = y \frac{P}{RT^g} c_p^{CO_2} \frac{\partial T^g}{\partial t} + (1-y) \frac{P}{RT^g} c_p^{N_2} \frac{\partial T^g}{\partial t} \end{aligned} \quad (8)$$

where

$$\frac{\partial q}{\partial t} > 0 \Rightarrow \delta_k = 1 \quad \text{and} \quad \frac{\partial q}{\partial t} < 0 \Rightarrow \delta_k = 0$$

$$\delta_k = 0 \Leftrightarrow \frac{\partial q^j}{\partial t} < 0$$

3.4. Solid phase Conservation of energy:

The adsorbent layer exchanges heat with the gas phase and metallic structure of exchanger. The adsorbent temperature can be calculated from the conservation of energy on the adsorbent layer.

$$h(T^g - T^a) - U(T^a - T^m) + \delta \frac{\partial q}{\partial t} (\delta_k \int_{T^a}^{T^g} c_p^{CO_2} dT + \Delta H) = \delta \frac{\partial(\rho_{adsorbent} c_p^a T^a)}{\partial t} \quad (9)$$

As it is concluded from equation 9, the adsorbent temperature depends on both gas and the temperature of exchanger structure. Assuming a quasi-steady state for exchanger metallic structure, the temperature of

exchanger structure can be calculated from the following equations:

$$m^0 c_p^w (T_{in}^w - T_{out}^w) = UA(T^m - T^a) \quad (10)$$

$$\Delta T_{LMTD} = \frac{T_{in}^w - T_{out}^w}{Ln \left(\frac{T_{in}^w}{T_{out}^w} \right)} = T^m \quad (11)$$

4. Initial and Boundary Conditions:

The initial and boundary conditions for the equations are summarized in Table 1, and the numerical value of constant parameters presented in those equations are adopted from literatures and are summarized in table 2.

Table.1. Initial and boundary equations for governing equations

Governing equation	Initial and boundary conditions	
	Adsorption step	Desorption step
Mole conservation of adsorbing component in bed gas phase, equation (1)	$y _{z,t=0} = 0$	$y _{z=0,t} = 0.13$
Mole conservation of adsorbing component in adsorbent layer gas phase, equation (2)	$q _{z,t=0} = 0$	
Total mole conservation Gas phase, equation (7)	$Q _{z=0,t} = Q_{in}$	$Q _{z=L,t} = 0$
Gas phase conservation of thermal energy Gas phase, equation (8)	$T^g _{z=0,t} = 298 K$	$T^g _{z,t=0} = 298 K$
Solid phase conservation of energy Solid phase, equation (9)	$T^a _{z,t=0} = 298 K$	

Table.2. Numerical value of parameters used in calculations

Parameter	value	reference
W, H, L [m]	0.5, 0.5, 2	
ϵ_b	0.25	
ϵ_m	0.25	
K_{s0} [s^{-1}]	0.165	
α	1.31	
$\rho_{adsorbent}$ [kg/m^3]	960	
q_{s0} [mole/kg]	1.29	
η	1.26	(Rezaei et al., 2014)
b_0 [1/pa]	0.8	
T_0 [K]	298	
ΔH [kJ/mole]	-112	
A, B	0.28, 1.32	
Q_{in} [m^3 STP/minutes]	2, 4, 6	
h [$W/m^2 K$]	10	
U [$W/m^2 K$]	50	(Bejan & Kraus, 2003)
P [pa]	101325	
C_p^a [j/ kg K]	1000	
m^0 [kg/min]	50	
C_p^w [j/kg K]	4178	
T_{in}^w [°C]	Cooling 25, 35, 45 Heating 80, 100, 120	
Duration of adsorption and regeneration steps [minutes]	10, 10	

5. Results and Discussion

The recovery¹, productivity² and purity³ of carbon dioxide separation are three interrelated parameters which vary with operating conditions such as feed flow rate, cooling water temperature and hot water temperature. To assess the effect of these important parameters on the performance of the proposed structure, a parametric study was run. As it is indicated, the mentioned separation cycle of CO₂ needs a heating step and a cooling step. To minimize the energy demand of such a process, it is necessary that the cycle work with waste heat or solar sources. The temperature of such resources normally ranges from 60 to 150 C, and it is desirable that cooling step be done at ambient temperature. Thus, the range of cooling was

selected from 25 C to 45C, and the range of heating was selected from 80 C to 120 C. All these parametric studies were done for the same cycle time (10 minutes adsorption step and 10 minutes desorption step).

5.1. Effect of Cooling Water Temperature

The effect of cooling water temperature on the recovery and purity and on the productivity is represented in figure 3 and figure 4 respectively. These figures show that as cooling water temperature increases, recovery, purity and productivity decrease. It is because of the reduction in equilibrium adsorption capacity and affinity due to the rise in the adsorbent temperature.

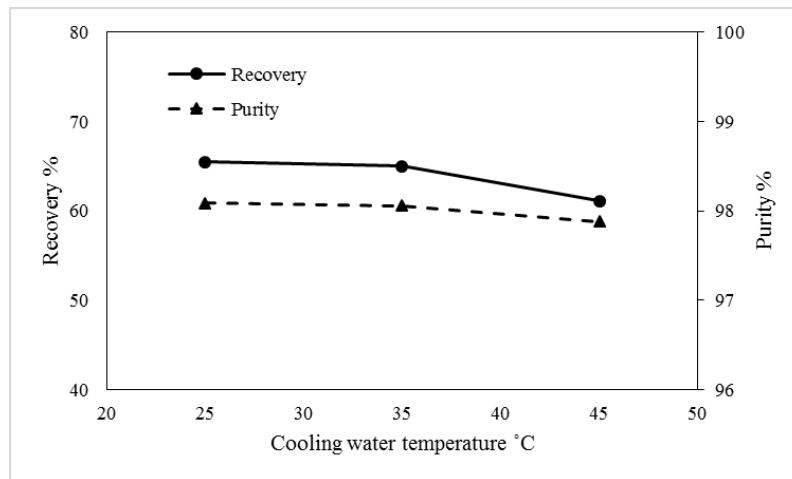


Figure.3. Effect of cooling water temperature on recovery and purity of carbon dioxide ($T_H=120$ C, $Q=6$ STP cubic meter/minutes).

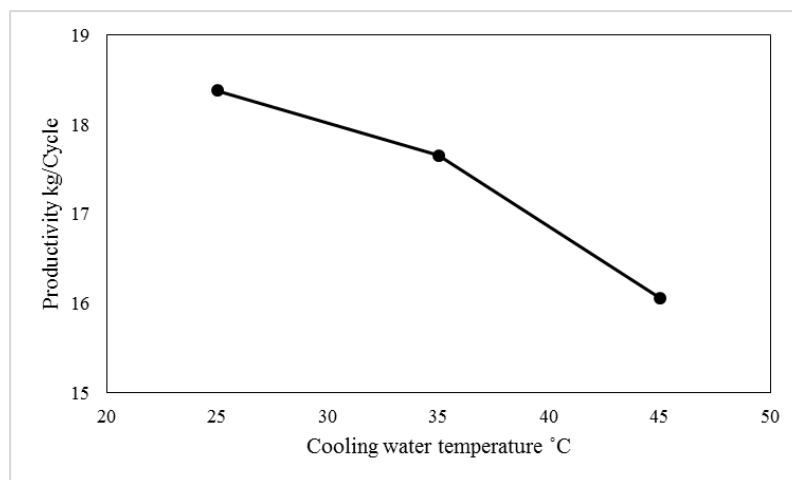


Figure.4. Effect of cooling water temperature on productivity of carbon dioxide ($T_H=120$ C, $Q=6$ STP cubic meter/minutes).

¹ kg of CO₂ that is separated in a cycle/ kg of CO₂ that is entered to the unit in a cycle

² kg of CO₂ that is separated in a cycle

³ Average mole fraction of separated CO₂ in a cycle

5.2. Effect of Hot Water Temperature

The figures 5 and 6 disclose the effect of hot water temperature on the performance of the system. As it is shown in these figures, by increasing the regeneration temperature all three factors increase. It is because of the better regeneration of the adsorbent at higher temperatures. When the temperature of the regeneration step increases, the amount of desorbed CO_2 increases.

5.3. Effect of Feed Flow Rate

Figure 7 and figure 8 explore the effect of feed flow rate on the performance of the proposed

bed. Figure 7 shows that by increasing the feed from $2 \text{ m}^3\text{STP}/\text{min}$ to $4 \text{ m}^3\text{STP}/\text{min}$, there is a small reduction in recovery and a moderate rise in purity; however, the increase in feed from 4 to $6 \text{ m}^3\text{STP}/\text{min}$ causes a sharp reduction in recovery, while the variation of purity is negligible. The trend of productivity is illustrated in figure 8. By increasing the feed flow rate from 2 to 4, the productivity increases; however, like purity, by increasing the feed from 4 to 6, there is no noticeable change in productivity.

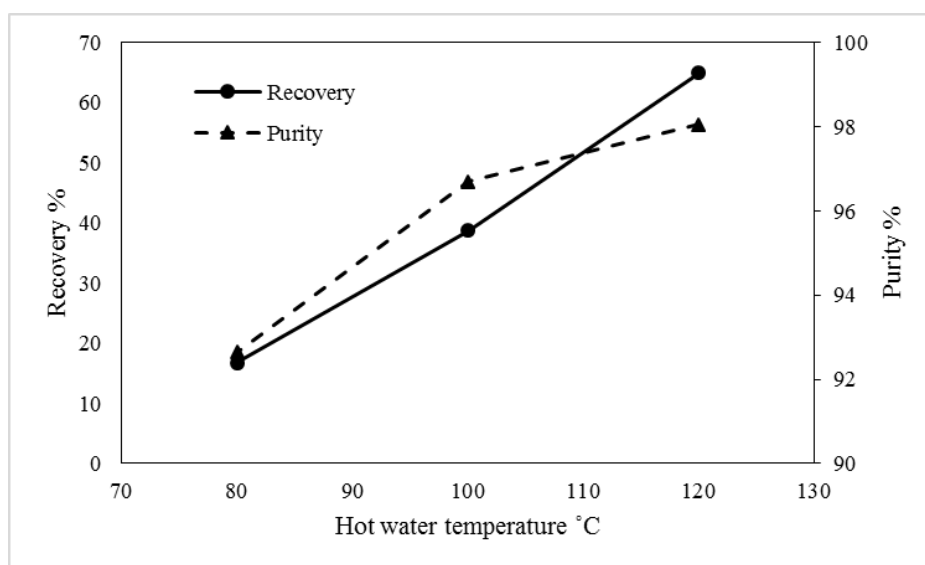


Figure.5. Effect of hot water temperature on recovery and purity of carbon dioxide ($T_c=35 \text{ C}$, $Q=6 \text{ STP cubic meter/minutes}$).

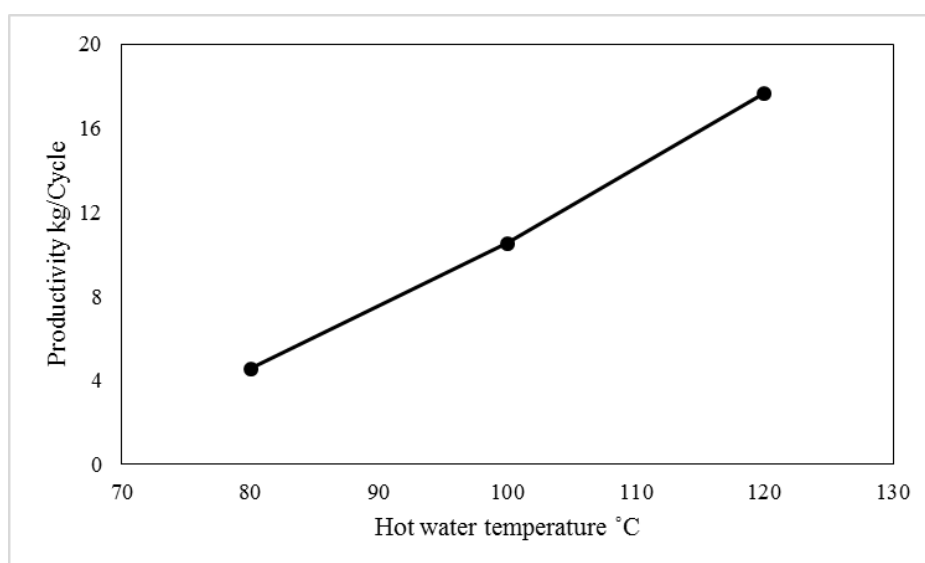


Figure.6. Effect of hot water temperature on productivity of carbon dioxide ($T_c=35 \text{ C}$, $Q=6 \text{ STP cubic meter/minutes}$).

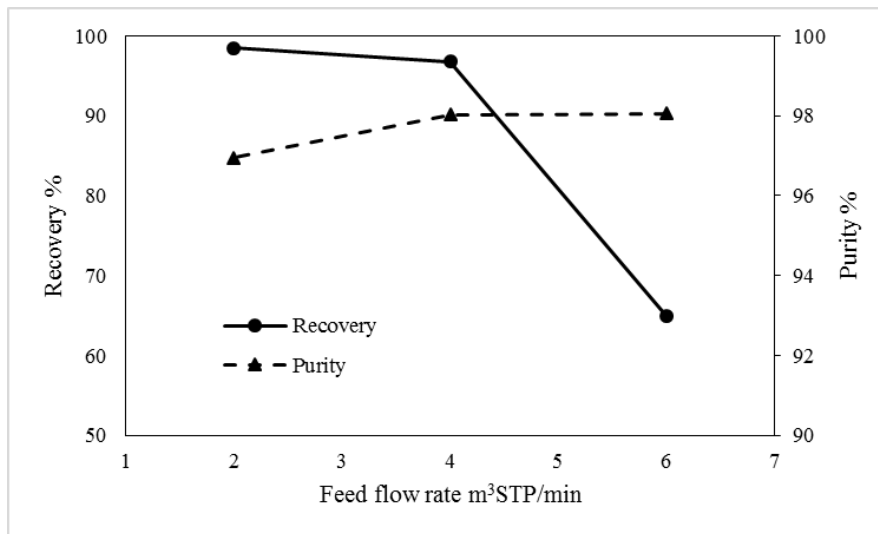


Figure.7. Effect of feed flow rate on recovery and purity of carbon dioxide ($T_C=35$ C, $T_H=120$ C).

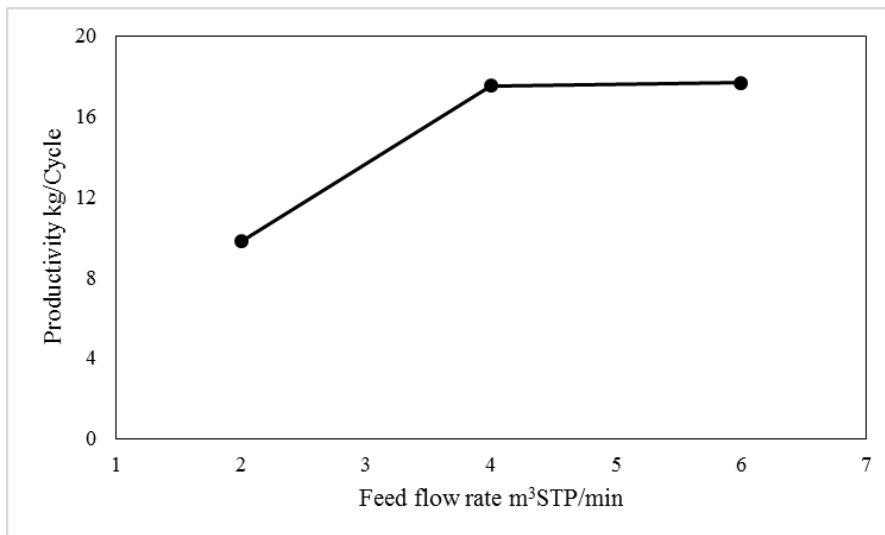


Figure.8. Effect of feed flow rate on productivity of carbon dioxide ($T_C=35$ C, $T_H=120$ C).

Table.3. Equilibrium time of proposed bed

Feed flow rate	2	4	6
Equilibrium time (S)	1222	611	407

These trends are well explained by equilibrium times of bed for different feed flow rates which are presented in table 3. It can be understood from this table that the equilibrium time for 2 cubic meter per minutes (STP) is much higher than the duration of the adsorption step. It means that a noticeable part of bed is unused in each cycle. Therefore, the recovery is high, but the recovered CO_2 will get diluted by N_2 presented in the bed. At feed flow rate of 6 m^3 STP/min, the equilibrium time is much lesser than the length of the adsorption step. It reveals that a part of the entered CO_2 exits the bed, and consequently the recovery is low.

5.4. Cyclic Simulation

In the previous section, the results of operating parameters on the performance of the system was presented. These results showed that when the flow rate is 4 normal cubic meter per minutes and the hot water temperature is 120 degree of centigrade, the recovery, productivity and purity are almost in their maximum values, i.e. 96%, 98%, 17.5 kg/cycle. However, the cooling water temperature did not change the performance of the system very much. Therefore, this condition was selected for further elaboration on cyclic simulation. In figure 9, the profile of average CO_2 loading and gas temperature at middle of the bed is shown for three last cycles of simulation.

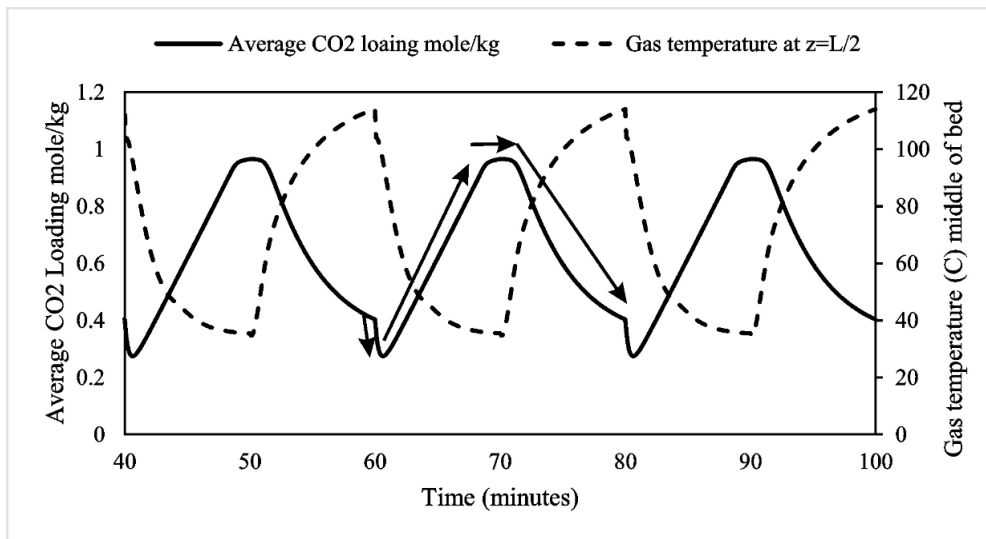


Figure.9. Profile of average CO₂ loading and gas temperature at $z=L/2$ versus time for three last cycles out of 5.

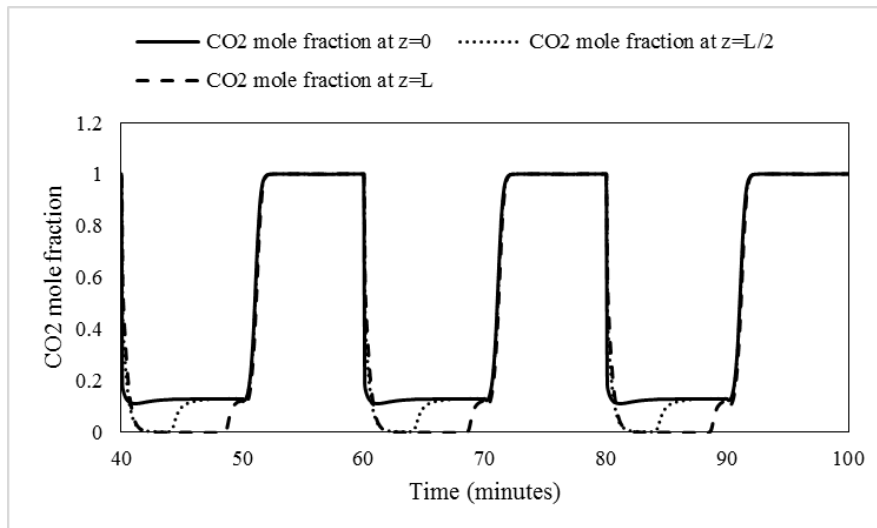


Figure.10. Profile of CO₂ mole fraction at $z=0$, $z=L/2$, and $z=L$ versus time for three last cycles out of 5.

The graph of average loading can be divided to 4 regions which are shown by 4 arrows. In the first part, a sharp reduction is shown in the average loading. At the beginning of the adsorption step, a fresh gas containing 13% CO₂ enters the bed, which causes a sharp reduction in CO₂ mole fraction along the bed (figure 10). Noting that the bed temperature is still high, this sharp reduction in the amount of CO₂ in gas phase causes further desorption of CO₂ from the adsorbents. The second part is the nearly linear increase of average loading versus time. In this part, the bed temperature is low enough to adsorb the CO₂, all of the entered CO₂ are adsorbed, and the outlet fraction is almost zero.

In the third part, the graph of average loading gets closely flat, which means no more adsorption is taking place. In fact, the bed is

almost in its equilibrium state with flowing gas, and the outlet mole fraction starts to rise (figure 10). The last part is the declining section of the graph which is caused by heating up the bed.

6. Conclusion

In this study, the performance of an adsorbent coated finned tube exchanger was studied numerically. The results show that this structure has a great potential for being applied in short cycle (or rapid) temperature swing adsorption. For the case of carbon capture with a simple cycle consisting of two steps, including adsorption and regeneration (without purging and sweeping), this structure can create high recovery and purity which are of interest in separation processes. It should be noted that finned tube exchangers are well developed to create minor pressure drop in

gas and liquid phase; thus, they are suitable structures for getting coated by adsorbent for the purpose of gas separation by Rapid Thermal Swing Adsorption.

References

- Bauer, J., Herrmann, R., Mittelbach, W., & Schwieger, W. (2009). Zeolite/aluminum composite adsorbents for application in adsorption refrigeration. *International Journal of Energy Research*, 33(13), 1233-1249. doi: 10.1002/er.1611
- Bejan, A., & Kraus, A. D. (2003). *Heat transfer handbook*. New York: J. Wiley.
- Boelman, E. C., Saha, B. B., & Kashiwagi, T. (1995). *Experimental investigation of a silica gel-water adsorption refrigeration cycle - The influence of operating conditions on cooling output and COP*. American Society of Heating, Refrigerating and Air-Conditioning Engineers, Inc., Atlanta, GA (United States).
- Bonnissel, M. P., Luo, L., & Tondeur, D. (2001). Rapid Thermal Swing Adsorption. *Industrial & Engineering Chemistry Research*, 40(10), 2322-2334. doi: 10.1021/ie000809k
- Clausse, M., Merel, J., & Meunier, F. (2011). Numerical parametric study on CO₂ capture by indirect thermal swing adsorption. *International Journal of Greenhouse Gas Control*, 5(5), 1206-1213. doi: <http://dx.doi.org/10.1016/j.ijggc.2011.05.036>
- Determan, M. D., Hoysall, D. C., & Garimella, S. (2012). Heat- and Mass-Transfer Kinetics of Carbon Dioxide Capture Using Sorbent-Loaded Hollow Fibers. *Industrial & Engineering Chemistry Research*, 51(1), 495-502. doi: 10.1021/ie201380r
- Fatemeh Hosseini, S., Reza Talaie, M., Aghamiri, S., Hasan Khademi, M., Gholami, M., & Nasr Esfahany, M. (2017). Mathematical modeling of rapid temperature swing adsorption; the role of influencing parameters. *Separation and Purification Technology*, 183, 181-193. doi: <http://dx.doi.org/10.1016/j.seppur.2017.03.017>
- Freni, A., Bonaccorsi, L., Calabrese, L., Capri, A., Frazzica, A., & Sapienza, A. (2015). SAPO-34 coated adsorbent heat exchanger for adsorption chillers. *Applied Thermal Engineering*, 82, 1-7. doi: <http://dx.doi.org/10.1016/j.applthermaleng.2015.02.052>
- Hefti, M., Joss, L., Bjelobrck, Z., & Mazzotti, M. (2016). On the potential of phase-change adsorbents for CO₂ capture by temperature swing adsorption. *Faraday Discussions*, 192(0), 153-179. doi: 10.1039/C6FD00040A
- Joss, L., Gazzani, M., & Mazzotti, M. (2017). Rational design of temperature swing adsorption cycles for post-combustion CO₂ capture. *Chemical Engineering Science*, 158, 381-394. doi: <http://dx.doi.org/10.1016/j.ces.2016.10.013>
- Lee, K. B., & Sircar, S. (2008). Removal and recovery of compressed CO₂ from flue gas by a novel thermal swing chemisorption process. *AIChE Journal*, 54(9), 2293-2302. doi: 10.1002/aic.11531
- Lively, R., Chance, R. R., Koros, W. J., Deckman, H., & Kelley, B. T. (2012). Sorbent fiber compositions and methods of temperature swing adsorption: Google Patents.
- Lively, R. P., Chance, R. R., Kelley, B. T., Deckman, H. W., Drese, J. H., Jones, C. W., & Koros, W. J. (2009). Hollow Fiber Adsorbents for CO₂ Removal from Flue Gas. *Industrial & Engineering Chemistry Research*, 48(15), 7314-7324. doi: 10.1021/ie9005244
- Marx, D., Joss, L., Hefti, M., & Mazzotti, M. (2016). Temperature Swing Adsorption for Postcombustion CO₂ Capture: Single- and Multicolumn Experiments and Simulations. *Industrial & Engineering Chemistry Research*, 55(5), 1401-1412. doi: 10.1021/acs.iecr.5b03727
- Merel, J., Clausse, M., & Meunier, F. (2008). Experimental Investigation on CO₂ Post-Combustion Capture by Indirect Thermal Swing Adsorption Using 13X and 5A Zeolites. *Industrial & Engineering Chemistry Research*, 47(1), 209-215. doi: 10.1021/ie071012x
- Mérel, J., Clausse, M., & Meunier, F. (2006). Carbon dioxide capture by indirect thermal swing adsorption using 13X zeolite. *Environmental Progress*, 25(4), 327-333. doi: 10.1002/ep.10166
- Restuccia, G., Freni, A., Russo, F., & Vasta, S. (2005). Experimental investigation of a solid adsorption chiller based on a heat exchanger coated with hydrophobic zeolite. *Applied Thermal Engineering*, 25(10), 1419-1428. doi: <http://dx.doi.org/10.1016/j.applthermaleng.2004.09.012>
- Rezaei, F., Subramanian, S., Kalyanaraman, J., Lively, R. P., Kawajiri, Y., & Realff, M. J. (2014). Modeling of rapid temperature swing adsorption using hollow fiber sorbents. *Chemical Engineering Science*, 113, 62-76. doi: <http://dx.doi.org/10.1016/j.ces.2014.04.002>
- Yong, L., & Wang, R. Z. (2007). Adsorption Refrigeration: A Survey of Novel Technologies. *Recent Patents on Engineering*, 1(1), 1-21. doi: 10.2174/187221207779814725
- Zhu, R., Han, B., Lin, M., & Yu, Y. (1992). Experimental investigation on an adsorption system for producing chilled water. *International Journal of Refrigeration*, 15(1), 31-34. doi: [http://dx.doi.org/10.1016/0140-7007\(92\)90064-2](http://dx.doi.org/10.1016/0140-7007(92)90064-2)

Nomenclature

A_b cross sectional area of bed (m^2)
 b adsorption affinity parameter (kPa^{-1}), center to center crossing distance between two adjacent fins of exchanger
 b_{ref} reference adsorption affinity parameter (kPa^{-1})
 K_{so} adsorption rate constant (1/s)
 n adsorption equilibrium parameter
 P Pressure (Pa), partial pressure of adsorbate
 q Adsorbing component concentration in solid phase ($mole/m^3$)
 q_s Saturation capacity of adsorbing component in solid phase ($mole/kg$)
 q^* equilibrium concentration of adsorbing component in solid phase ($mole/m^3$)

Q feed flow rate ($mole/s$)
 R gas constant
 T_g gas temperature (K)
 T_a adsorbent temperature (K)
 T^m temperature of fins (K)
 t time (s)
 U interstitial velocity (m/s)
 y mole fraction
 z axial distance in bed (m)
 Greek letters
 a Adsorption rate constant
 ϵ_b void fraction of bed
 ϵ_m fraction of bed occupied by fins of exchanger
 $\rho_{adsorbent}$ particle skeleton density (kg/m^3)
 θ fractional surface coverage